JOURNAL OF MATERIALS SCIENCE: MATERIALS IN MEDICINE 13 (2002) 443–448

Electrochemical impedance spectroscopy study of high-palladium dental alloys. Part II: Behavior at active and passive potentials*

D. SUN
Section of Oral Biology, College of Dentistry, The Ohio State University, Columbus, OH, USA
P. MONAGHAN, W. A. BRANTLEY†, W. M. JOHNSTON
Section of Restorative Dentistry, Prosthodontics and Endodontics, College of Dentistry, The Ohio State University, PO Box 182357, Columbus, OH, USA 43218-2357
E-mail: brantley.1@osu.edu

Electrochemical impedance spectroscopic (EIS) analyses were performed on three high-palladium alloys and a gold–palladium alloy at active and passive potentials in five electrolytes that simulated body fluid and oral environmental conditions. All four alloys were previously found to have excellent corrosion resistance in these *in vitro* environments. Before performing the EIS analyses, alloy specimens were subjected to a clinically relevant heat treatment that simulated the firing cycles for a dental porcelain. It was found that the EIS spectra varied with test potential and electrolyte. Diffusional effects, related to the dealloying and subsequent surface enrichment in palladium of the high-palladium alloys, along with species adsorption and passivation, were revealed at both active and passive potentials, although these effects were more evident at the passive potentials.

1. Introduction

In the first part of this study, electrochemical impedance spectroscopic (EIS) analyses demonstrated that representative high-palladium alloys, whether based on Pd–Cu–Ga or Pd–Ga systems, had similar corrosion current densities [1]. Additionally, the corrosion current densities of the high-palladium alloys were comparable to those of a gold–palladium alloy. Corrosion resistances for all four tested alloys were high, and the best interfacial circuit model was a modified Randles circuit, in which a constant phase element replaced the capacitor. The high nobility of these alloys was thought to be responsible for their excellent *in vitro* corrosion resistance. Moreover, palladium enrichment of the high-palladium alloy surface, caused by selective dealloying of less noble constituents, is an established mechanism that would yield a more noble surface with time [2, 3].

Generally, EIS analyses are performed at the corrosion potential of the alloy, but these studies can be performed at other potentials to investigate processes that are not evident at the open-circuit potential [4]. A separate study, using these same alloys and potentiodynamic polarization tests [5], confirmed that the representative high-palladium alloys possessed active–passive characteristics, by examining the variation in corrosion current density with applied potential. The objective of this study was to use EIS techniques to investigate the same representative high-palladium alloys and the gold–palladium alloy at potentials anodic to their corrosion potentials to identify any corrosion mechanisms not revealed in the previous experiments. The rationale for using these elevated potentials was based upon their previously determined [1, 5] very high corrosion resistances. The alloys were tested in the clinically relevant heat-treated condition that simulated the firing cycles used for application of porcelain for metal–ceramic restorations [6]. A previous study suggested that the *in vitro* corrosion processes for the high-palladium alloys do not seem to be affected by this heat treatment [7].

2. Materials and methods

As in Part I of this study [1], the electrochemical behavior of three high-palladium alloys [the Pd–Cu–Ga alloys, Freedom Plus and Liberty, and the Pd–Ga alloy, Legacy], and the Au–Pd alloy, Olympia, was examined in five electrolytes simulating body fluid and oral environmental conditions: aqueous 0.09% and 0.9% NaCl solutions, Fusayama solution, N_2-deaerated aqueous 0.09% NaCl solution ($pH = 4$) and N_2-deaerated Fusayama solution ($pH = 4$). All four alloys are manufactured by J. F.

* A part of this study was presented at the 30th annual meeting of the American Association for Dental Research, Chicago, IL, March 2001.
†Author to whom all correspondence should be addressed.

Jelenko & Co., Armonk, NY, USA. Test specimens of 12 mm diameter and 1.3 mm original thickness were prepared by standard dental laboratory procedures, metallographically polished to 0.05 μm final surface roughness, and given a heat treatment that simulated the firing cycles for a dental porcelain [1].

The EIS tests were performed on three specimens of each heat-treated alloy after stepping the voltage to a selected elevated potential, relative to the open-circuit potential (OCP), based upon data previously collected from cyclic polarization tests [5, 8]. Two selected potentials for EIS analysis were used for each alloy/electrolyte combination, representing active (lower potential) and passive (higher potential) corrosion behavior. A 2.5 cm × 2.5 cm platinum plate served as the counter electrode, and a saturated Ag | AgCl reference electrode was used. After the current reached quasi-steady state (about 10 min after the potential step), a sinusoidal voltage varying from +10 to −10 mV about the selected potential was impressed upon the specimen through the range of 10 kHz to 0.01 Hz.

The current was collected and analyzed for magnitude and phase compliance with the voltage, and the real (in-phase) impedance (Z') and imaginary (90° out-of-phase) impedance (Z'') were determined at sampled frequencies. The values of Z' and Z'' at the sampled frequencies for the various alloy/electrolyte combinations and the selected elevated potentials were plotted as Nyquist diagrams, where values of the imaginary and real impedances are given on the vertical and horizontal axes, respectively [1]. The total impedance (Z) is related to the real and imaginary components of impedance by the expression $Z = [(Z')^2 + (Z'')^2]^{1/2}$. While the Nyquist diagrams show the values of the two impedance components, it is most useful to discuss the alloy behavior as the testing frequency is varied. The mathematical relationship between each impedance component (Z' and Z'') and frequency is not straightforward. In the figures to follow that present the experimental EIS results, the lower-frequency range corresponds to the higher-impedance range, and the higher-frequency range corresponds to the lower-impedance range.

3. Results

Figs. 1–5 present Nyquist diagrams of the EIS spectra at selected elevated potentials for the four heat-treated alloys in the five electrolytes. In each electrolyte, the individual spectra for the three specimens of the same alloy were very similar. The EIS spectra of these alloys at the open circuit potential have been discussed in Part I, where it was noted that at the corrosion potentials the Nyquist diagrams were truncated arcs [1].

At the lower potentials in the active range for the four alloys in the five electrolytes, each diagram generally consisted of an arc at high frequencies (low impedances), coupled to a line at low frequencies (high impedances), as shown in Figs. 1(A)–5(A). However, while this appearance was observed in Fig. 1(A) for the Olympia Au–Pd alloy at the active potential in 0.9% NaCl solution, the Nyquist diagrams for the three high-palladium alloys at their active potentials in this electrolyte had a completely different appearance. These three diagrams had similar and lower slopes compared to the Olympia alloy in the highest-frequency (lowest-impedance) range, and arcs curving towards the vertical Z'' axis at lower frequencies (higher impedances). Distinctly different electrochemical responses were observed in Fig. 1(A) at the lower frequency range for each high-palladium alloy (Liberty, Legacy and Freedom Plus).

At the passive, higher potentials investigated for the four alloys in the five electrolytes, three general observations could be made about the Nyquist diagrams in Figs. 1(B)–5(B):

1. For alloys tested in 0.9% NaCl solutions, each diagram consisted of an arc at high frequencies (low impedances), a line at medium frequencies, and another arc at low frequencies (high impedances), as shown in

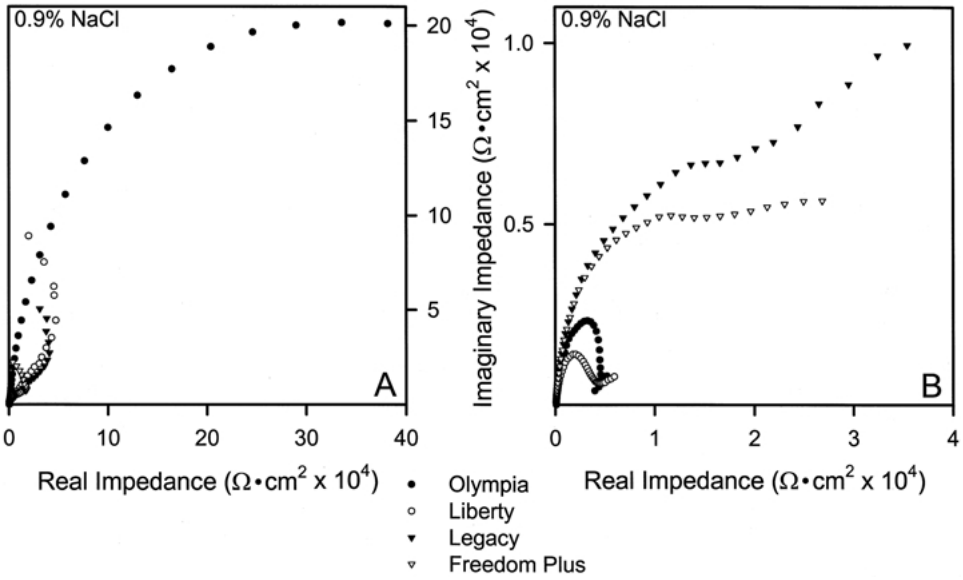

Figure 1 Nyquist plots for heat-treated alloys in 0.9% NaCl at elevated potentials vs. OCP: (A) Potentials representing active behavior: Olympia 200 mV; Liberty 450 mV; Legacy 400 mV; Freedom Plus 300 mV. (B) Potentials representing passive behavior: Olympia 500 mV; Liberty 700 mV; Legacy 650 mV; Freedom Plus 650 mV.

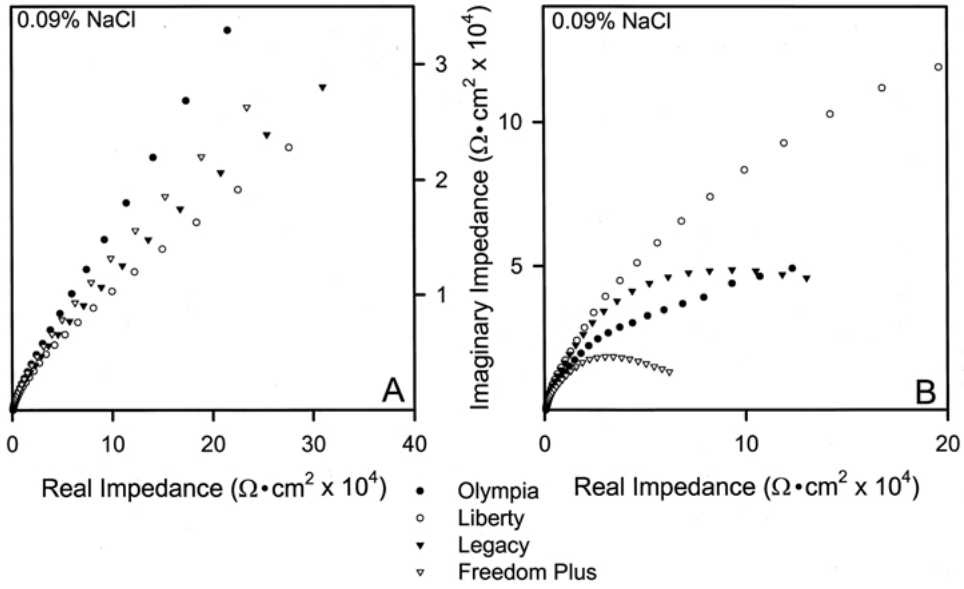

Figure 2 Nyquist plots for heat-treated alloys in 0.09% NaCl at elevated potentials vs. OCP: (A) Potentials representing active behavior: Olympia 300 mV; Liberty 300 mV; Legacy 300 mV; Freedom Plus 200 mV. (B) Potentials representing passive behavior: Olympia 550 mV; Liberty 550 mV; Legacy 550 mV; Freedom Plus 600 mV.

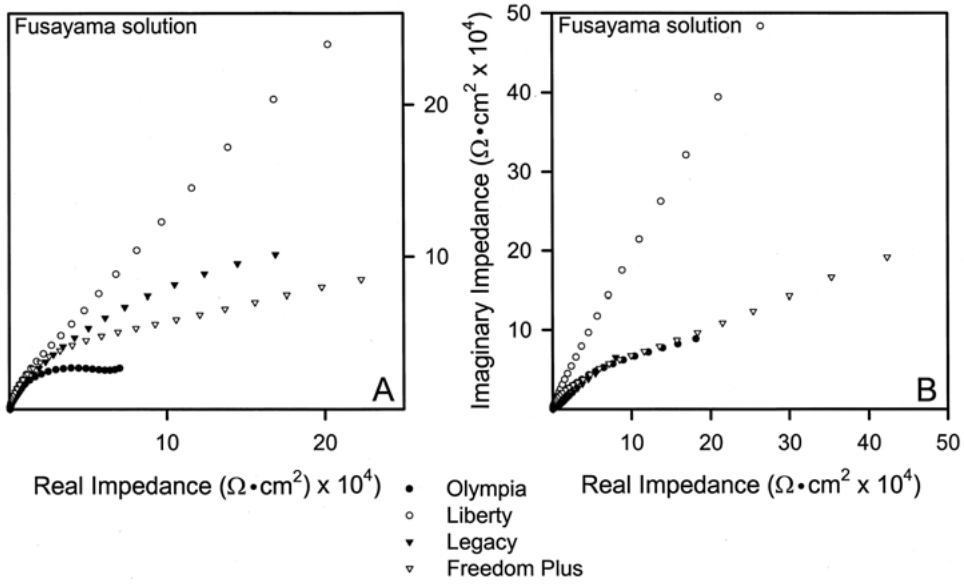

Figure 3 Nyquist plots for heat-treated alloys in Fusayama solution at elevated potentials vs. OCP: (A) Potentials representing active behavior: Olympia 70 mV; Liberty 200 mV; Legacy 200 mV; Freedom Plus 200 mV. (B) Potentials representing passive behavior: Olympia 550 mV; Liberty 500 mV; Legacy 600 mV; Freedom Plus 800 mV.

Fig. 1(B). For the Olympia alloy in this electrolyte, the low-frequency arc strongly curved toward the horizontal Z' axis, whereas the low-frequency arc for the Liberty high-palladium alloy first curved toward and then away from the Z' axis.

2. For alloys tested in 0.09% NaCl solutions, whether aerated or deaerated, each diagram commonly consisted of a simple arc at higher frequencies (lower impedances), followed by a straight line at lower frequencies (higher impedances), as shown in Figs. 2(B) and 4(B). For the Freedom Plus alloy in 0.09% NaCl solution, this linear portion of the diagram at lower frequencies (higher impedances) curved toward the horizontal Z' axis, as shown in Fig. 2(B), unlike the electrochemical responses of the other three alloys. In deaerated 0.09% NaCl solution, the diagram for the Olympia alloy at low frequencies (high impedances) had a very different appearance from that for the other three alloys, consisting of an arc that curved strongly towards and becoming essentially tangent to the horizontal Z' axis, as shown in Fig. 4(B).

3. For alloys tested in the Fusayama solutions, whether aerated or deaerated, each diagram consisted of an arc at high frequencies coupled to a line at low frequencies, as shown in Figs. 3(B) and 5(B). The diagrams for the Olympia, Freedom Plus and Legacy alloys were nearly coincident in the aerated Fusayama solution and widely separated from the diagram for Liberty, as shown in Fig. 3(B). Fig. 5(B) shows that, while the electrochemical responses for the four alloys were nearly the same in deaerated Fusayama solution at high frequencies (low impedances), there was consider-

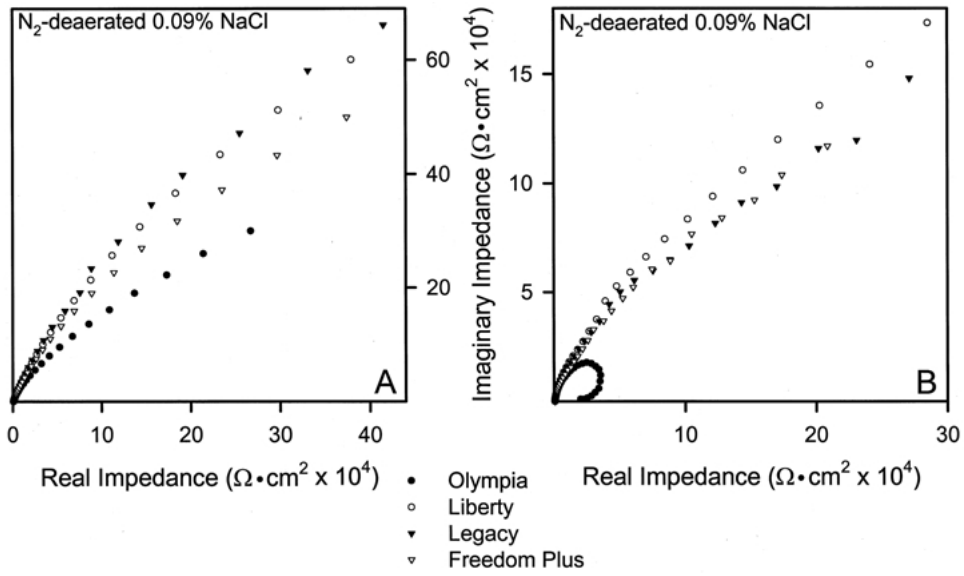

Figure 4 Nyquist plots for heat-treated alloys in deaerated 0.09% NaCl solution at elevated potentials vs. OCP: (A) Potentials representing active behavior: Olympia 300 mV; Liberty 150 mV; Legacy 200 mV; Freedom Plus 200 mV. (B) Potentials representing passive behavior: Olympia 550 mV; Liberty 550 mV; Legacy 550 mV; Freedom Plus 600 mV.

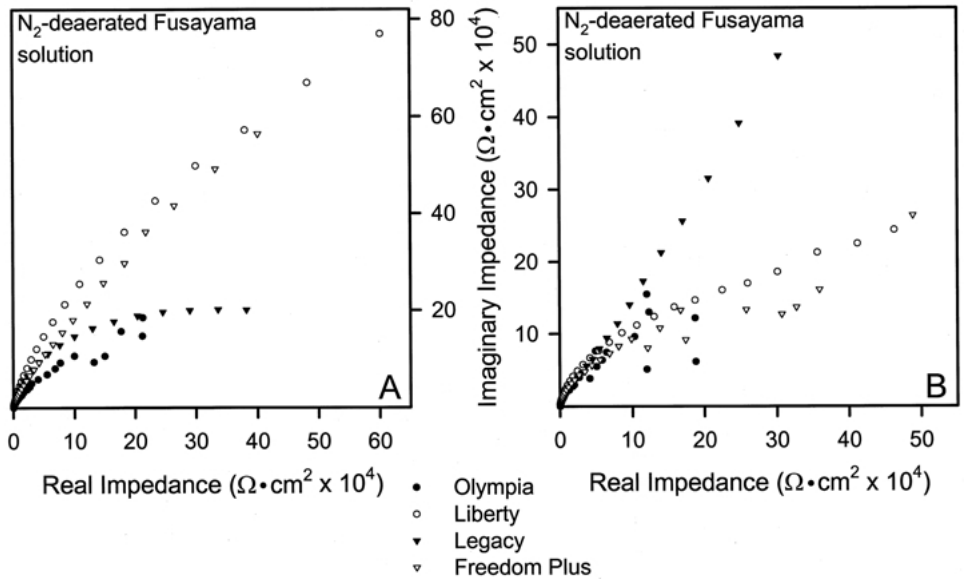

Figure 5 Nyquist plots for heat-treated alloys in deaerated Fusayama solution at elevated potentials vs. OCP: (A) Potentials representing active behavior: Olympia 300 mV; Liberty 300 mV; Legacy 200 mV; Freedom Plus 200 mV. (B) Potentials representing passive behavior: Olympia 550 mV; Liberty 550 mV; Legacy 600 mV; Freedom Plus 550 mV.

able scatter in the diagrams for the Olympia and Freedom Plus alloys at low frequencies (high impedances). The electrochemical behavior of Legacy in this electrolyte, where the Nyquist diagram was nearly a straight-line segment for all frequencies, was distinctly different from that for the other three alloys at low frequencies (high impedances).

4. Discussion

The EIS spectra for the four alloys in Figs. 1–5 are derived from responses to specific electrochemical mechanisms at the selected potentials that govern corrosion in the given electrolytes [1]. These include both Faradaic processes (involving transfer of charge), such as metal ionization and formation of passive films, and non-Faradaic processes (involving no transfer of charge), such as adsorption of species, reorientation of surface molecules, and diffusion effects. The study of electrochemical phenomena at the elevated potentials used in this investigation is highly relevant to corrosion processes in the oral environment, where the potential range of interest has been reported [9] to be from -100 to $+300$ mV (vs. SCE).

The initial portions (which are nearest the origin) of the diagrams in Figs. 1–5 show that the high-frequency (low-impedance) electrochemical responses of the three high-palladium alloys and the gold–palladium alloy are very similar in each of the five electrolytes at elevated potentials relative to their open-circuit potentials. Differences in the electrochemical responses of the four alloys at the elevated potentials become apparent at

lower frequencies (higher impedances). This result is to be expected, since there is insufficient time available at lower frequencies for electrochemical processes such as diffusion and oxide dissolution, that have substantial time-dependence, as discussed later. Such processes would be expected to differ among the four alloys evaluated, which have varying elemental compositions. In contrast, the electrochemical process occurring at the high-frequency (low-impedance) range in Figs. 1–5 would be from electron transport and not associated with diffusional processes.

Because the thermal oxidation behavior is considerably different for the Liberty and Legacy high-palladium alloys [10], it would be expected that substantial differences would occur in the electrochemical oxidation behavior of all four alloys investigated in this study. These differences would be particularly apparent at the elevated potentials in the passive range in Figs. 1(B)–5(B), where formation of surface oxide films occurs.

Fig. 1(B) suggests that, because of the higher impedance response of Legacy and Freedom Plus in the 0.9% NaCl solution at low frequencies, the passive oxide film on these alloys may be thicker and perhaps more continuous than the passive oxide films on the Liberty and Olympia alloys in this electrolyte. The low-frequency response in Fig. 4(B) for Olympia in the N_2-deaerated 0.09% NaCl solution also suggests that the passive oxide film is not as protective in this electrolyte, due to perhaps lower thickness or less continuity, compared to the passive oxide films on the three high-palladium alloys. Detailed study of the composition, thickness and continuity of the oxide films that form in the five electrolytes at the passive and active potentials will require the combined use of techniques such as atomic force microscopy, scanning tunneling microscopy, Auger electron spectroscopy, X-ray photoelectron spectroscopy, ellipsometry, and transmission electron microscopy.

The general similarity among the Nyquist plots at high frequencies (low impedances) for the four alloys in Figs. 1–5 suggests that the primary mechanism for corrosion protection is their high-noble character and that differences in the alloy microstructures have secondary roles. (The nobility of these alloys is based upon the sum of their gold and palladium contents.) The three high-palladium alloys contain greater than 75 wt % palladium and 2 wt % gold [11, 12], and both the Liberty and Legacy alloys have a unique submicron tweed structure observed by transmission electron microscopy (TEM) [13, 14]. A similar tweed structure would be expected in the Freedom Plus high-palladium alloy. This submicron structure is found in both the as-cast and simulated porcelain-firing heat-treated conditions of the high-palladium alloys [13], and is thought to be very stable and possibly resistant to corrosion [14]. In contrast, the higher-nobility alloy, Olympia, which contains approximately 52% gold and 38% palladium, has a very different microstructure [15] compared to the high-palladium alloys; TEM observations have shown that this alloy does not contain a tweed structure [16].

Investigation at potentials anodic to the corrosion potential has provided some insight into possible mechanisms that govern the corrosion properties of these alloys. The linear portion of the Nyquist diagram at low frequencies is often referred to as a diffusion tail [17, 18], and this feature can be seen in Figs. 1–5 for both active and passive potentials. Dealloying has been proposed as one of the major corrosion mechanisms of the high palladium alloys [2, 3]. The less-noble elements, such as copper, gallium, tin and indium, are depleted from the alloy surface, leading to palladium-enrichment. The corrosion kinetics for this process would be under diffusion control, as metal atoms migrate through the enriched palladium surface.

In the passive region, an oxide film forms on the alloy surface, which blocks further corrosion. Adsorption of species in solution, such as hydrogen ions, proteins, and oxygen ions, is known to occur with palladium; palladium is often used as a catalytic surface for chemical reactions, including protein hydrogenation [19–22]. Mucin is a component of the Fusayama solution [23], and two of the electrolytes used in this study had pH values of 4, indicating that the hydrogen ion concentration was 10^{-4} M, which would be very acidic for a biological environment. Adsorption of these species would be diffusion-controled and, once adsorbed onto the palladium surface, these species would inhibit the release of metallic ions into the corrosion medium. The effects of diffusion control seemed to be more pronounced for the alloys at their passive potential, rather than at their active potential, as previously noted. Detailed investigation of these surface phenomena during corrosion of the high-palladium alloys requires the use of Auger electron spectroscopy and X-ray photoelectron spectroscopy.

Ferrous alloys, such as mild steel, and nonferrous metals, such as copper, are usually investigated at their corrosion potentials with EIS techniques [24, 25]. However, their corrosion resistances are significantly lower than the noble alloys tested in the present study. Since the corrosion potential is a measure of the electrochemical free energy of the alloy to corrode in its environment [26], a small perturbation in voltage at the corrosion potential of these noble alloys during EIS analysis would provide little information about the corrosion control processes. However, when a higher impressed potential is used as the starting condition for the EIS analysis, the small ripple in potential produces significantly stronger data. These impressed potentials cause reactions of interest to occur and contribute to the impedance characteristics of the system, which can then be measured and identified.

5. Conclusions

Variations in the electrochemical impedance of three representative high-palladium alloys and a gold–palladium alloy were found with respect to both the potential and the electrolyte used for EIS analyses. These alloys had been subjected to clinically relevant heat treatment simulating the complete firing cycles for dental porcelain. In addition to corrosion control by their innate nobility, the potentially stable tweed structure and the formation of a passivating film on the alloy surface, diffusion control may play an important role in corrosion properties of the high-palladium alloys. Based upon the

results from other studies, this diffusion control may be related to the early loss of less-noble elements, which yields a palladium-enriched surface that is more corrosion-resistant than the original alloy surface condition. The present results suggest that high-palladium alloys have corrosion properties at least equivalent to those of the gold–palladium alloy evaluated, and they should be expected to provide excellent clinical performance.

Acknowledgments

Support for this research was received from Grant DE10147, National Institute of Dental and Craniofacial Research, Bethesda, MD, USA, and from a University Faculty Seed Grant. We thank Professor Gerald S. Frankel, Department of Materials Science and Engineering, The Ohio State University for helpful comments during this study.

References

1. D. SUN, P. MONAGHAN, W. A. BRANTLEY and W. M. JOHNSTON, *J. Mater. Sci.: Mater. Med.* **13**(5) (2002) 435–442.
2. V. GOEHLICH and M. MAREK, *Dent. Mater.* **6** (1990) 103.
3. I. KAWASHIMA, D. BERZINS, N. K. SARKAR and A. PRASAD, *J. Dent. Res.* **78** (1999) 236 (Abstr. No. 1045).
4. I. EPELBOIN, M. KEDDAM and H. TAKENOUTI, *J. Appl. Electrochem.* **2** (1972) 71.
5. D. SUN, P. MONAGHAN, W. A. BRANTLEY and W. M. JOHNSTON, *J. Prosthet. Dent.* **87** (2002) 86.
6. E. PAPAZOGLOU, W. A. BRANTLEY, A. B. CARR and W. M. JOHNSTON, *ibid.* **70** (1993) 386.
7. Z. CAI, S. G. VERMILYEA and W. A. BRANTLEY, *Dent. Mater.* **15** (1999) 202.
8. D. SUN. Master of Science thesis, The Ohio State University, Columbus, OH, USA (2000).
9. M. M. VRIJHOEF, P. R. MEZGER, J. M. VAN DER ZEL and E. H. GREENER, *J. Dent. Res.* **66** (1987) 1456.
10. S. J. KERBER, T. L. BARR, G. P. MANN, W. A. BRANTLEY, E. PAPAZOGLOU and J. C. MITCHELL. *J. Mater. Eng. Perform.* **7** (1998) 334.
11. W. A. BRANTLEY, Z. CAI, A. B. CARR and J. C. MITCHELL, *Cells Mater.* **3** (1993) 103.
12. Q. WU, W. A. BRANTLEY, J. C. MITCHELL, S. G. VERMILYEA, J. XIAO and W. GUO, *ibid.* **7** (1997) 161.
13. Z. CAI, W. A. BRANTLEY, W. A. T. CLARK and H. O. COLIJN, *Dent. Mater.* **13** (1997) 365.
14. S. V. NITTA, W. A. T. CLARK, W. A. BRANTLEY, R. J. GRYLLS and Z. CAI, *J. Mater. Sci.: Mater. Med.* **10** (1999) 1.
15. S. G. VERMILYEA, E. F. HUGET, J. M. VILCA, *J. Prosthet. Dent.* **44** (1980) 294.
16. W. H. GUO, W. A. BRANTLEY and W. A. T. CLARK (unpublished research).
17. F. MANSFELD, H. SHIH, H. GREENE and C. H. TSAI, in ''Electrochemical Impedance: Analysis and Interpretation'', edited by J. R. Scully, D. C. Silverman and M. W. Kendig (ASTM STP 1188, American Society for Testing and Materials, Philadelphia, 1993) p. 37.
18. R. G. KELLY, A. J. YOUNG and R. C. NEWMAN, in ''Electrochemical Impedance: Analysis and Interpretation'', edited by J. R. Scully, D. C. Silverman and M. W. Kendig (ASTM STP 1188, American Society for Testing and Materials, Philadelphia, 1993) p. 94.
19. J. RAMACHANDRAN and C. BEHRENS, *Biochim. Biophys. Acta* **496** (1977) 321.
20. J. A. COOK, W. J. WHEELER, G. W. BECKER and M. C. SMITH, *Anal. Biochem.* **198** (1991) 379.
21. D. J. BARABINO and C. DYBOWSKI, *Solid State Nucl. Magn. Reson.* **1** (1992) 5.
22. Y. J. HUANG, H. P. WANG, C. T. YEH, C. C. TAI and C. Y. PENG, *Chemosphere* **39** (1999) 2279.
23. T. FUSAYAMA, T. KATAYORI and S. NOMOTO, *J. Dent. Res.* **42** (1963) 1183.
24. J. D. SCANTLEBURY, K. N. HO and D. A. EDEN, in ''Electrochemical Corrosion Testing'', edited by F. Mansfeld and U. Bertocci (ASTM STP 727, American Society for Testing and Materials, Philadelphia, 1981) p. 187.
25. W. H. SMYRL, in ''Electrochemical Corrosion Testing'', edited by F. Mansfeld and U. Bertocci (ASTM STP 727, American Society for Testing and Materials, Philadelphia, 1981) p. 198.
26. J. M. WEST, in ''Basic Oxidation and Corrosion'', 2nd edn. (Ellis Horwood, Chichester, U.K., 1986) p. 58.

Received 12 September
and accepted 22 October 2001